

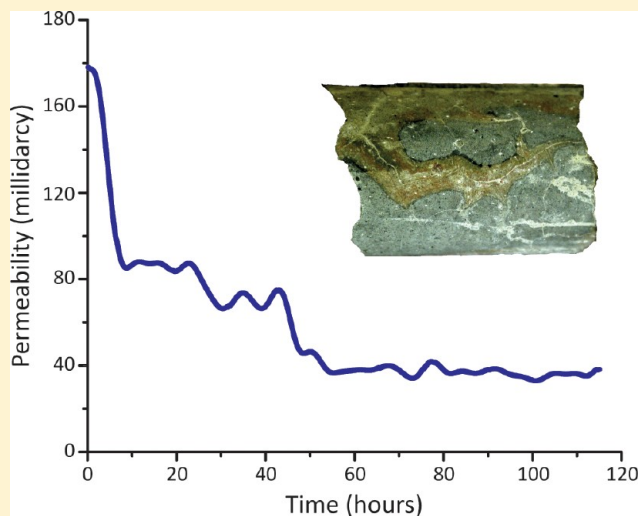
Experimental Evaluation of Wellbore Integrity Along the Cement-rock Boundary

Dennis L. Newell* and J. William Carey

Earth and Environmental Sciences, Los Alamos National Laboratory, Los Alamos, NM

S Supporting Information

ABSTRACT: Leakage of CO₂ and brine from geologic storage reservoirs along wellbores is a major risk factor to the success of geologic carbon sequestration. We conducted multiphase [supercritical (sc)CO₂-brine] coreflood experiments that simulate a leakage pathway along the cement/rock interface. A composite core constructed of oil-well cement and siltstone separated by a simulated damage zone (defect) containing ground cement and siltstone was flooded with brine + scCO₂ at 10 MPa and 60 °C parallel to the defect. During coinjection of scCO₂, the effective brine permeability decreased from ~200 to 90 mD due to transition to two-phase flow and then further declined to 35 mD. CO₂ injection resulted in a pH drop from 11 to 4 and carbonate-undersaturated conditions in the produced brine. Microscopy revealed leaching and erosion along the defect, a carbonation front extending 5 mm into the cement, parallel to the damage zone, and no change in the dimensions of the defect. Carbonation of cement does not appear to explain the permeability drop, which is attributed to the migration and reprecipitation of alteration products derived from cement within the defect. This study shows the potential for self-limiting flow along wellbore defects despite flow of aggressive scCO₂-brine mixtures.



INTRODUCTION

The viability of geologic carbon sequestration requires demonstrating that CO₂ can be stored for long periods (ca. 1000 years) in subsurface targets such as deep saline aquifers or depleted hydrocarbon reservoirs. Studies suggest that wells that penetrate these targets are one of the most significant potential leakage pathways for CO₂ back to the surface or into shallow drinking water aquifers.^{1–3} Although well integrity will be important at any sequestration site, it is critical to the utilization of depleted oil and gas reservoirs and other regions with numerous well penetrations. Properly designed wells isolate the subsurface through the use of a Portland cement seal between the steel casing and the caprock. At abandonment, the inside of the wells are commonly sealed with cement plugs. Long-term concerns about well integrity are driven by the well-known chemical reactivity of CO₂ with both Portland cement and steel.^{4–6} One key question is determining the conditions under which these reactions are deleterious in deep wellbore environments.

It is clear from field studies that Portland cement and carbon steel can survive decades in CO₂-rich environments without significant deterioration of material properties.^{5,7} These studies have shown that it is not the susceptibility of these materials to reactions with CO₂ that is of greatest concern, but it is the existence of defects within the cement or gaps between steel

and cement and cement and caprock that provide potential leakage pathways. (See Gasda et al.⁸ for an excellent graphical representation of potential leakage pathways in a wellbore, including defects between the cement and caprock.) At both a CO₂ enhanced oil recovery (EOR) operation⁵ and a commercial natural CO₂ producing reservoir,⁷ migration of CO₂ occurred along these interfaces.

With this understanding, the focus of our research on wellbore integrity is on determining whether these defects exist and on the chemical and mechanical evolution of the defect in response to flow of CO₂ or changes in reservoir stress. Transmissive interfaces may occur because of defects in the original well construction or due to subsequent geomechanical effects that separate interface bonds. Once a defect forms, fluid flow has the potential to increase its transmissivity through dissolution reactions, but also has the potential to self-heal due to mineral precipitation. A full understanding of the wellbore problem requires an integrated geochemical and geomechanical

Special Issue: Carbon Sequestration

Received: March 23, 2012

Revised: May 30, 2012

Accepted: June 4, 2012

Published: June 4, 2012



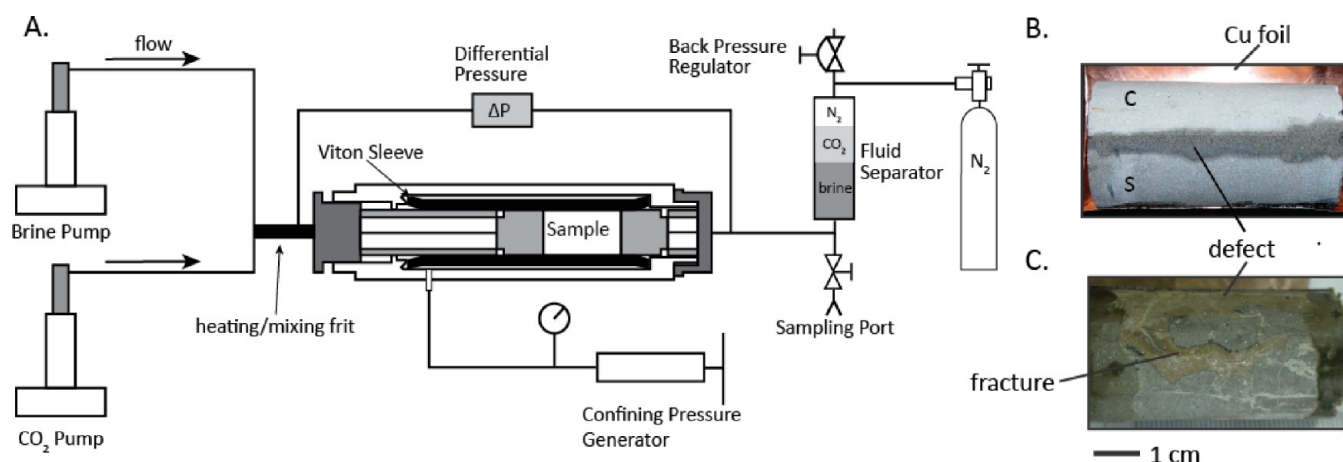


Figure 1. (A) Schematic showing the main components of the coreflood experimental system. Brine and high-pressure CO₂ mix are delivered to the core using ISCO pumps. A back-pressure regulator governs the pore pressure, and a fluid separator allows for geochemical sampling. (B) Composite core sample preparation: Cement and siltstone are held in place by copper foil. A 0.25 cm damage zone (defect) between the cement (c) and siltstone (s) was constructed of a mixture of siltstone and cement. (C) Postexperiment view of the cement-side of the core. The end-caps are darkened from epoxy used to seal the copper foil. The exterior surface shows unaltered, gray cement and a distinct, orange region of carbonated cement. The center line of the orange finger in the middle of the photo is the locus of a crack that facilitated CO₂ migration. At the top of the image, the carbonated region extends to the defect, which may also have allowed some CO₂ to migrate beneath the foil.

Table 1. Aqueous Chemistry Analyses, Concentrations in mg/kg^a

hours	Al	Ca	Cl	Fe	HCO ₃	K	Mg	Na	Si	SO ₄	Sr	pH lab	pH (in situ)	CO ₂ total
0.0	0.1	346	1106	0.1	100	116	19	263	0.5	161	0.2	8.1	8.1	100
0.9	9.0	84	1339	0.6	320	282	1.0	1128	28	582	0.3	9.9	10.7	21
4.5	2.4	212	1124	0.4	180	191	0.8	513	10	236	0.9	9.7	10.2	nd
19.2	0.3	822	1112	3	2111	133	52	388	46	188	2.2	6.6	nd	nd
20.2	0.4	725	1053	2	1950	133	45	355	38	197	1.7	7.2	4.3	77 860
26.9	0.1	643	1110	3	1267	127	36	319	34	161	1.5	6.5	4.2	53 177
42.4	0.2	637	1110	7	1099	125	35	313	33	160	1.3	6.4	4.0	67 613
44.9	0.2	556	1043	0.8	1073	134	34	322	29	162	1.2	6.4	4.0	60 435
51.9	0.4	586	1041	2	1104	123	37	303	30	180	1.3	6.4	3.9	78300
65.4	0.1	595	1072	5	1108	123	32	284	31	164	1.2	6.4	4.1	50 626
68.7	0.2	587	1038	8	1078	125	32	286	29	156	1.1	6.4	4.0	58 303
77.3	0.4	522	1234	2	807	127	32	296	26	174	1.0	6.2	3.8	60 968
90.0	0.1	519	1044	4	781	120	31	282	29	157	1.0	6.2	3.6	87 408
91.6	0.3	481	1205	5	709	120	30	275	25	163	0.9	5.9	3.5	79 610
99.9	0.4	463	1053	11	627	117	29	265	22	154	0.8	6.1	3.6	82 755
114.4	0.4	499	1057	16	730	118	32	272	29	161	1.0	6.1	3.7	68 211
115.0	0.3	496	1205	4	728	123	33	279	26	173	0.9	6.4	4.0	45 167

^aTime zero = initial brine. Both the lab pH and calculated in situ pH are reported; see text for details. HCO₃ is measured at lab conditions and pH. CO₂ total is the total inorganic carbon composition of the in situ fluid and was obtained by coulometry and reflects a combination of dissolved and gas phase CO₂. CO₂ injection starts at 4.7 h with breakthrough observed at 19.2 h.

model capable of representing fluid flow and chemical reaction and the impacts of stress on the development of defects.

The goal of this study was to experimentally evaluate the evolution of the cement-caprock interface during CO₂ leakage. Defects at the cement-caprock interface may exist because of inadequate removal of drill cuttings, formation of a drilling mud filter cake, formation damage during drilling, or geomechanical stresses. In these cases, a porous pathway may exist for flow of CO₂ and brine from the reservoir to shallower environments. We conducted a bench-scale coreflood experiment on a composite Portland cement-caprock sample to determine the magnitude of CO₂-brine flow and the potential for geochemical reactions to modify the permeability of flow along this defect.

EXPERIMENTAL METHODS

The experiment was conducted using a coreflood device shown in Figure 1A. The sample consisted of half-cylinders of wellbore cement (50:50 mixture of Class H Portland cement and fly ash, 3 wt % bentonite, water/cement ratio = 0.57, cured for 1 week at 65 °C, and held at room temperature in 100% humidity for 1 year) and a siltstone from the Graneros shale. The siltstone consists primarily of quartz, clay and calcite cement. To simulate a defect between the caprock and wellbore cement, an artificial damage zone was constructed by placing between half-cylinders of cement and siltstone a mixture of crushed hydrated cement (20%) and siltstone (80%), both with a 125–250 μm grain size. The damage zone was 0.25 cm thick resulting in a core 2.54 cm diameter and 5.1 cm length (Figure 1B). The composite sample was wrapped in copper foil to prevent

migration of supercritical (sc)CO₂ out of the core into the sealing sleeve and placed in a Viton sleeve and inserted into a Hassler-style coreholder. The experiment was conducted at 60 °C with a confining pressure of 18 MPa. The experiment consisted of initially flowing just low salinity brine (0.4 M, Table 1) into the sample to establish steady-state temperature and pressure conditions followed by coinjecting a mixture of scCO₂ and brine into the sample. The two fluids were mixed and brought to temperature at the face of the core using a heated, sintered stainless-steel frit as a mixing chamber. The experiment was run in constant-flow mode with an applied back-pressure of 10 MPa. For comparison, the confining and pore pressure in a field study at a natural CO₂ producer was 30 and 10 MPa, respectively.⁷ Three different brine-CO₂ flow rates were used (at ambient *T* and experimental *P*): 0.15/0.048, 0.20/0.06, and 0.25/0.08 mL/min. Variable flow rates were used to (1) prevent exhaustion of fluid reservoirs overnight and (2) to evaluate changing flow rates on pressure drop across the sample. The highest flow rate was used during the day when fluid reservoirs could be readily replenished. Based on the Duan and Sun⁹ equation of state, the brine-CO₂ flow rates equate to in situ volumetric CO₂/brine ratios of ~0.49, which ensured 2-phase conditions with coexisting scCO₂ and brine. The pressure drop across the core was measured with a differential pressure transducer to evaluate changes in permeability during the experiment. Seventeen fluid samples were collected as they exited the core for chemical analysis. Aqueous samples were analyzed by ion chromatography for anions, and inductively coupled plasma optical emission spectrometry (ICP-OES) or mass spectrometry (ICP-MS) for cations. Due to the impacts of CO₂ degassing during sampling, in situ pH values were calculated. The pH was calculated using PHREEQC¹⁰ by taking the ex situ pH and bicarbonate alkalinity and then “titrating” in CO₂ to reach the total in situ inorganic carbon measured by coulometry; this produces both the in situ pCO₂ and pH.¹¹

RESULTS

Pressure and Permeability. The experiment was conducted for 115 h with a total of 1461 mL of brine and 1380 mL of CO₂ injected at 60 °C and 10 MPa. Due to the low permeability of the cement and the siltstone, the majority of the flow was assumed to have occurred along the damage zone between the materials. This region had a volume defined by 0.25 × 2.54 × 5.08 cm (3.23 cm³) and a porosity of ~40% through which 1700 pore-volumes of mixed fluid passed. The measured pressure drop across the core varied between 14 and 62 kPa (2 and 9 psi) (Supporting Information (SI) Figure S1). Each day, the experiment was briefly stopped and the fluid reservoirs were recharged. This resulted in a small discontinuity in the pressure readings.

Prior to coinjection of CO₂, differential pressure measurements were steady. Initial values were about 17 kPa and quickly fell to 7 kPa before recovering to 21 kPa. This is interpreted as resulting from rearrangement and compaction of the defect contents, possibly with some chemical reaction between the brine and minerals. Co-injection of CO₂ and brine results in a much noisier differential pressure reading as the back-pressure regulator has a variable response to the very different viscosities of brine and CO₂. Although the readings are noisy, there is a clear increase in differential pressure with time (SI Figure S1).

Using the Darcy equation and appropriate in situ densities and viscosities,¹² effective permeability was calculated based on

the cross-sectional area of the defect (0.25 × 2.54 cm). The single phase intrinsic permeability (*k*) of this zone determined with brine was approximately 200 mD (Figure 2). Upon

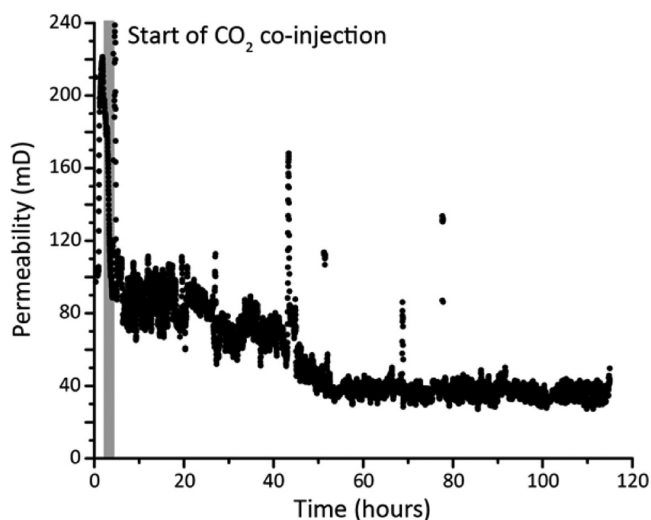


Figure 2. Running 10 min average cement-siltstone interface brine permeability data. For this calculation flow was assumed to be confined to the defect only. Note that the pressure record (SI Figure S1) and calculated permeability is smooth prior to CO₂ injection and noisy during 2-phase flow.

coinjection of CO₂, the effective permeability of brine dropped to ~90 mD equating to a relative permeability (k_{brine}/k) of ~0.45 (Figure 2). The effective permeability of CO₂ for this same period was ~16 mD, giving a relative permeability (k_{CO_2}/k) of ~0.08. At around 45 h, the effective permeability of brine and CO₂ decreased again to a steady value with an average of 35 and 7 mD, respectively.

Mineralogical Observations. Following the experiment, the core sample was removed from the copper jacket and a textural and mineralogical study was conducted. Evidence for CO₂ reaction with cement was immediately visible on the external surface of the core (Figure 1C). Copper foil was used to prevent fluid migration outside the core, but the interface region (defect) and a crack in the surface of the cement appear to have facilitated minor flow/diffusion of CO₂ between the copper foil and core. The orange discoloration of the cement in response to CO₂ exposure is characteristic of cement carbonation (e.g., ref 5). It is interesting to note that despite curing conditions free of stress, the cement contains minute fractures that allow penetration of CO₂.

The core was impregnated with blue-dyed epoxy (to reveal porosity) and slabbed for thin-section preparation. At thin-section scale, some material had been removed from the inlet during CO₂-brine injection, but the outlet did not show similar large-scale erosion features (Figure 3 A,B). It is also apparent that substantial porosity existed along the defect with distinct, small-scale channels at the siltstone interface and within the defect. The sections also clearly revealed the presence of a carbonation front in the cement (Figure 3A). This resulted from diffusion of CO₂ from the inlet face, from the defect, and from the outlet face into the cement to a depth of about 5 mm during the course of the 115 h experiment. There were no obvious indications of CO₂-induced alteration within the siltstone.

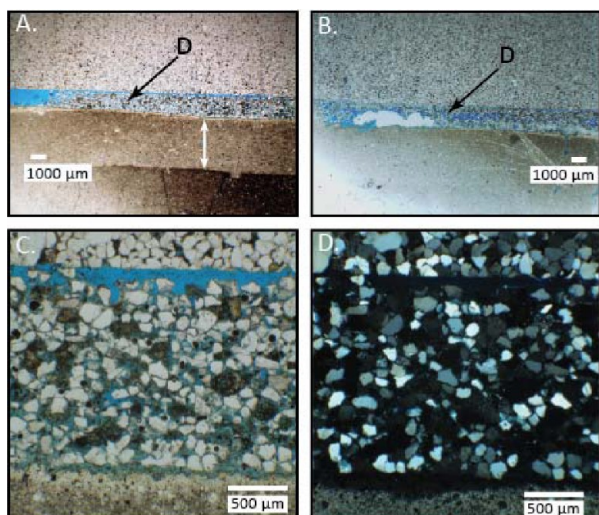


Figure 3. Thin sections of core showing inlet (far left in A) and outlet (far right in B) of defect (D + black arrow), with the siltstone above and cement below. Note the erosion and loss of material in the interface at the inlet, but not at the outlet. The band in the cement (arrow in A) is the carbonation front and reflects the diffusion distance of CO_2 into cement (about 5 mm). Photomicrographs in plane (C) and cross-polarized light (D) showing interface region and siltstone above and cement below. Note development of enhanced porosity at the interface with siltstone.

Observations by optical microscopy of thin sections show the presence of a distinct, high-porosity channel at the boundary between the siltstone and the damage zone (Figure 3C, D). The siltstone appears unaffected by the flooding process. The defect contains siltstone grains (principally quartz) and patches of Portland cement phases. Evidence exists for physical dislocation (note regions of high porosity in Figure 3A, B) and alteration (dissolution and chemical reaction) of the cement phases as seen in the brown patches in the defect (Figure 3C). The boundary between the Portland cement and the damage zone is sharp and lacks textures indicating erosion or other defect-widening processes. The Portland cement has a distinct morphological zone (<0.5 mm in width) adjacent to the damage zone, where the carbonated cement appears denser and richer in carbonate than cement further away from the defect. The carbonation front is a sharp boundary separating a region of abundant carbonate (particularly evident as brightly transmitting light and high-order interference colors in crossed-polarized light) from a region lacking any evidence for carbonate (SI Figure S2A). In places, fractures in the cement allowed further penetration of CO_2 into the cement as evidenced by the presence of carbonate (SI Figure S2B).

Scanning electron microscopy (SEM) study of the unaltered Portland cement showed typical cement textures with hydrated and partially hydrated cement grains, ettringite and finely distributed porosity (Figure 4A). In backscattered electron (BSE) images, the carbonation front is marked by a dense, carbonate-rich zone, approximately 100 μm in width (Figure 4B). The front is characterized by a lack of porosity, which may have impeded further diffusion of CO_2 into the cement interior. In some places, the dense front is cracked and may reflect the significant volume change associated with cement phase carbonation reactions or the effects of decompression at the end of the experiment. Within the carbonated zone, calcite is evident as a pore-filling material, ettringite is absent, and there

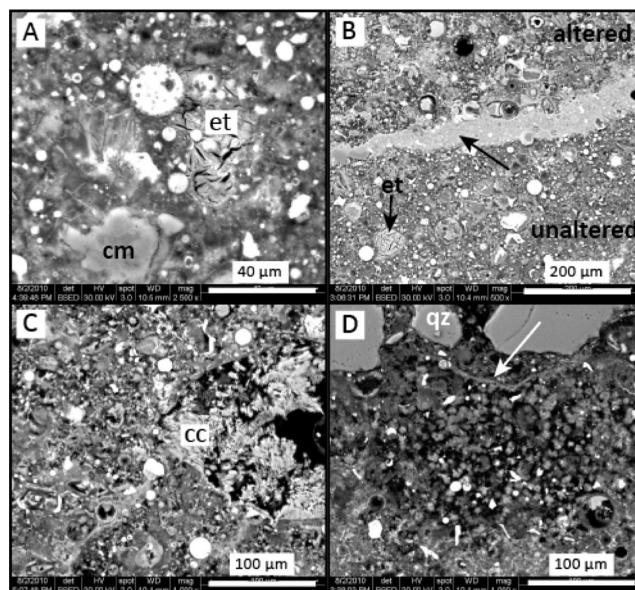


Figure 4. (A) Backscatter electron (BSE) image of unaltered cement. et = ettringite – note “tiger stripe” pattern, cm = nearly fully hydrated cement grain—hydration gives the cement grains a patchy gray color and is seen as thin gray hydration rims, smaller bright white circles are fly ash, black regions are pores. (B) The carbonation front (indicated with arrow) between carbonated cement (top) and unaltered cement (bottom). The carbonation front is calcite-rich and has low porosity. (C) Carbonated region cement showing increase in porosity and a pore partially filled with calcite (cc)—crystalline bright pore lining and filling material. Note the lack of ettringite in the carbonated cement (B, C). (D) BSE image of the contact (indicated with arrow) between the carbonated cement (bottom) and the defect. Quartz (qz) grains in the damage zone appear as large, smooth, light gray grains.

is a qualitative increase in cement porosity (Figure 4C). In some locations pores filled with carbonate may have been formerly occupied by now dissolved ettringite. While the Portland cement showed distinct evidence of reactions of CO_2 , the quartz-rich siltstone showed no obvious signs of CO_2 -induced dissolution or precipitation reactions at SEM scale. In contrast, dissolution of Portland cement phases in the damage zone resulted in the dislocation of siltstone particles and the formation of a significant void space in some regions, especially evident at the inlet. SEM observation of the contact between the Portland cement and the damage zone indicates a <100 μm zone with qualitatively increased porosity possibly indicating dissolution of cement phases (Figure 4D).

Chemistry of Fluids. Following CO_2 coinjection, a large increase in HCO_3^- , Ca, Mg, Sr, and Si was observed in the effluent (SI Figure S3; Table 1). With time, the concentration of these elements decreased. In contrast, the concentration of iron increases in an irregular fashion throughout the experiment. The concentrations of Ca, Sr, and Mg are highly correlated with the bicarbonate concentration (Figure 5). Prior to CO_2 injection, the solution pH is alkaline (~ 10 – 11) due to contact with the cement. After coinjection, the calculated in situ pH drops rapidly and equilibrates to values around 4 toward the later portion of the experiment (SI Figure S4). There is evidence for some reaction between the CO_2 -brine and copper foil based on fluid concentration rising from <1 ppm to ~ 30 ppm for most of the experiment before falling to <10 ppm near the termination of the experiment. No other evidence of Cu related reactions were observed.

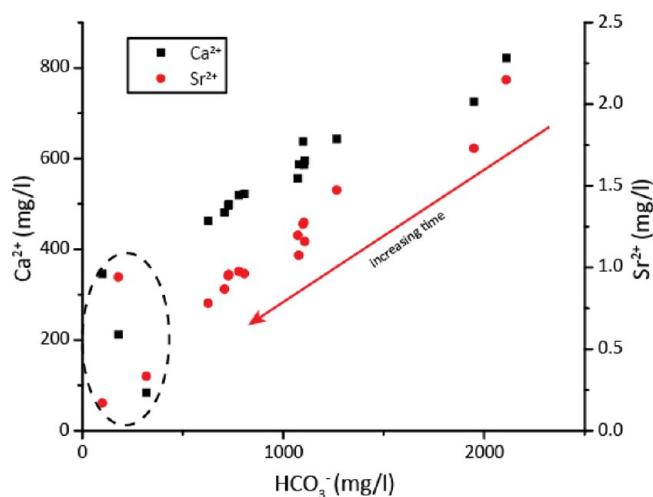


Figure 5. Correlation of Ca and Sr with bicarbonate (HCO_3^-). Pre- CO_2 samples are in the circled region. After application of CO_2 , concentrations started high and then decreased in a strongly correlated pattern. The arrow indicates that the concentration of Ca, Sr and HCO_3^- decreases with increasing time.

The geochemistry was evaluated using PHREEQC¹⁰ and the solution compositions in Table 1. Calculations were done at 60 °C and at 10 MPa CO_2 pressure for samples collected after CO_2 injection. Calculated mineral saturation indices show supersaturation of aluminum-bearing minerals (kaolinite, gibbsite, dawsonite etc.; Figure 6). Quartz was near saturation

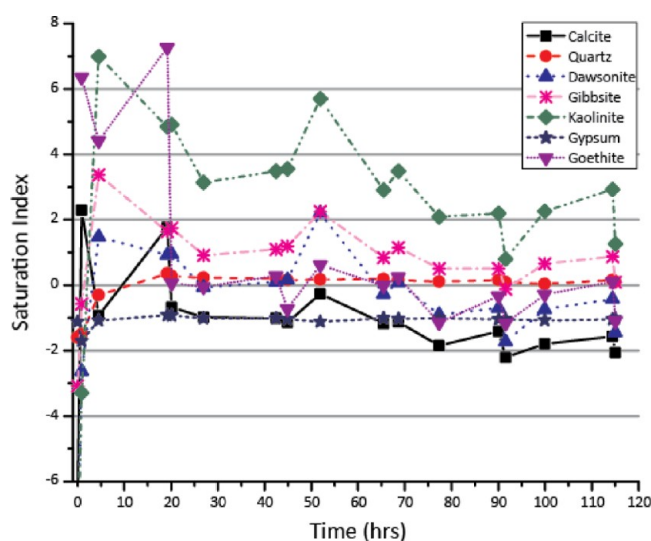


Figure 6. Calculated mineral saturations based on measured concentration of aqueous samples at temperature 60 °C using only bicarbonate content for the first three samples and an assumed CO_2 pressure of 10 MPa for the remaining samples.

throughout the experiment, while calcite and gypsum were undersaturated. Goethite, a ferric iron hydroxide, is also near saturation, but these results are sensitive to the assumed redox conditions in the experiment.

DISCUSSION

The experiment was designed to simulate a defective interface between cement and caprock in a wellbore that penetrates a geologic CO_2 sequestration reservoir. The wellbore defect was

composed of a mixed crushed assemblage of caprock and hydrated cement and represented a wellbore with poorly cleared drilling debris. A scCO_2 -brine mixture was pushed through the composite system at a rate of 0.3–0.5 mL/min. The scCO_2 portion of this flow was 0.14–0.24 mL/min. For comparison, this CO_2 flow is 4–40× faster than potential leakage rates that can be calculated from a natural CO_2 producer with a wellbore permeability between 1 and 10 mD (inferred over a single 3 m interval).^{7,13} The high laboratory rates were chosen to facilitate significant reaction over a reasonable amount of time. Under these conditions, the damage zone was eroded by fluid flow at the inlet but dislocation of the material and precipitation of cement residue toward the outlet resulted in a net decrease in permeability of the defect. This occurred despite the fact that the solution remained undersaturated with respect to carbonates and cannot be attributed to carbonate precipitation. Textural observations of the damage zone indicate the dislocation and redistribution of material was driven by dissolution reactions that removed material. Thus we believe that slower flow rates would also remove material, although possibly resulting in smaller permeability changes.

The cement was carbonated to 5 mm away from the defect, but there was no observed effect of CO_2 on the caprock, and thus it was not possible to estimate the depth of penetration of CO_2 into the caprock. Cement carbonation appears to have qualitatively increased the porosity of the Portland cement, but did not appear to increase permeability. Any permeability change to the cement was overshadowed by changes in the defect where permeability significantly decreased over the experiment. Thus we conclude that flow remained focused along the defect. In BSE images the maximum extent of carbonation into the cement is marked by a $\sim 100\ \mu\text{m}$ wide dense carbonation front. A similar front was observed by⁵ in a sample of carbonated cement retrieved from a well with 30 years of CO_2 -EOR operation but was not found by⁷ in a carbonated sample of a cement-fly ash mixture also with 30 years of potential CO_2 exposure. Similar results were observed in experimental studies on various cement formulations exposed to scCO_2 .^{14–16} They also found distinct reaction fronts in pure cements and no front (and faster penetration of CO_2) in cement with fly ash admixtures. Modeling studies have predicted a similar alteration front from the defect as seen in experiments that includes a zone altered to silica gel, followed by a calcite band and then unaltered cement.^{5,17,18} However,¹⁷ predicted eventual calcite precipitation downstream in the defect, which was not observed experimentally. This is likely due to the model using CO_2 -saturated water (not two-phase CO_2 -brine flow) which resulted in downstream depletion of CO_2 and eventual calcite-saturated conditions in the defect, whereas in this experiment the two-phase solution remained calcite undersaturated (Figure 6). The presence of the carbonate-rich front within the Portland cement suggests a degree of self-healing that protects some cement from further CO_2 intrusion through the deposition of dense carbonate.

The experimental results clearly show the impacts of channeled flow through the interface and support the concept that interface flow is the most significant leakage mechanism in wellbore systems.⁵ The textural observations show the effects of two-phase flow of scCO_2 and brine through the interface region and with penetration of CO_2 into cement occurring primarily by diffusion. It is assumed that CO_2 also diffuses into the caprock, although evidence of this was not observed in this

study. Although flow is strong in this study compared to field analogs, we did not observe significant widening of the interface region despite the fact that pure scCO₂-brine fluids were introduced at the inlet. It is difficult to extrapolate these experimental results to very long time periods; however, it is clear from this study as well as the results of a study conducted on cement-casing interfaces¹⁹ that cement is not easily eroded by flow of high-pressure CO₂-saturated fluids.

Perhaps the most intriguing result is the decrease in interface permeability observed during the experiment. This appears to be due to migration of fines and due to redistribution of dissolved cement phases (e.g., alumina hydroxides and amorphous silica, Figure 3) and occurred despite the maintenance of calcite-undersaturated conditions. The results add to other studies that show that at least under some conditions, wellbore interfaces have some self-healing capacity. Carey et al.¹⁹ observed precipitation of corrosion scale (FeCO₃) in the interface between cement and casing, and Huerta et al.²⁰ and Liteanu and Spiers²¹ observed a decrease in permeability associated with healing of fractures in cement.

Although the experiment was not designed specifically for observations of relative permeability, two-phase flow along the 200 mD defect at a CO₂ fractional flow rate of 0.5 resulted in a relative permeability of CO₂ and brine of 0.08 and 0.45, respectively. The initial permeability decrease is attributed to two-phase flow, but the subsequent drop to steady state is interpreted as a net change in the intrinsic permeability resulting from redistribution of minerals in the defect. This may also have been accompanied by a change in CO₂ saturation within the defect that could have contributed to the change in permeability. The reduction in brine/CO₂ relative permeability is similar to changes observed by Perrin and Benson²² at an equivalent CO₂ fractional flow rate from experiments on a 450 mD sandstone. These authors also measured fluid saturation by X-ray tomography, and for this fractional flow rate, the brine saturation was approximately 75%.

The changes in aqueous chemistry observed in the experiment reflect the contact of fresh CO₂-brine mixtures with the reactive interface material. Initially, rapid dissolution of cement phases occurs leading to a spike in the Ca, Mg, Sr, and Si concentration that is balanced by significant bicarbonate. Additionally, Ca, Mg, and Sr show a strong, positive correlation with bicarbonate (Figure 5). This covariation and the decline in concentration with time could indicate precipitation of a Mg–Sr-bearing calcite along the defect that is removing these elements and bicarbonate from solution. However, aside from carbonation in the cement, precipitation of carbonate minerals is not observed in the defect. Alternatively, this behavior likely arises because as the alteration front progresses into the cement, CO₂ is consumed during carbonation and cations (e.g., Ca²⁺) and bicarbonate are released to solution (e.g., refs 16,17). The propagation of the alteration front into the cement is limited by CO₂ diffusion, and thus the reactive surface area in the altered cement will drop with time, decreasing the release of cations and bicarbonate to solution similar to the observed chemical variation. This explanation is supported by geochemical modeling that indicates the solution remains undersaturated to calcite, and by observations of the cement showing that the alteration front progression was limited to 5 mm from the defect. Although not observed, geochemical modeling also suggests precipitation of Al bearing mineral phases (e.g., dawsonite), but this is likely to be spurious as similar results have been observed in other experiments (e.g., ref 23).

Many studies have evaluated the carbonation process in terms of wellbore leakage and our observations are generally consistent (e.g., ref 3); however, only a few address the impact to permeability of a wellbore defect.^{19–21,24,25} While significant, these experimental results do not yet prove that self-healing of wellbore defects happens in all cases. Field observations also indicate that this process does not always occur. Observations by Carey et al.⁵ at a CO₂-EOR site showed potential self-healing by deposition of carbonate in fractures and along interfaces. In contrast, Crow et al.⁷ did not observe evidence for self-healing mineralization at a natural CO₂ producer, but also did not see evidence for increased permeability. To establish self-healing as a predictable process, more definitive field observations are needed and a greater range of experiments need to be conducted.

■ ASSOCIATED CONTENT

Supporting Information

Additional figures available (Figures S1–S4). This material is available free of charge via the Internet at <http://pubs.acs.org>.

■ AUTHOR INFORMATION

Corresponding Author

*Phone: 505-667-1110; fax: 505-665-3285; e-mail: dnewell@lanl.gov

Notes

The authors declare no competing financial interest.

■ ACKNOWLEDGMENTS

We thank the CO₂ Capture Project (www.co2captureproject.org), a research partnership of major energy companies, for financial support, and Walter Crow for discussions and comments. The manuscript greatly benefited from three anonymous reviews.

■ REFERENCES

- (1) IPCC. *IPCC Special Report on Carbon Dioxide Capture and Storage*; Prepared by Working Group III of the Intergovernmental Panel on Climate Change: New York, 2005; p 442.
- (2) FutureGen. *Final Risk Assessment Report for the FutureGen Project Environmental Impact Statement*; Technical Report Contract No. DE-AT26-06NT42921; FutureGen Project, 2007; p 398.
- (3) Zhang, M.; Bachu, S. Review of integrity of existing wells in relation to CO₂ geological storage: What do we know? *Int. J. Greenhouse Gas Control* **2011**, *5*, 826–840.
- (4) Han, J.; Carey, J. W.; Zhang, J. A coupled electrochemical-geochemical model of corrosion for mild steel in high-pressure CO₂-saline environments. *Int. J. Greenhouse Gas Control* **2011**, *5*, 777–787.
- (5) Carey, W. J.; Wigand, M.; Chipera, S. J.; WoldeGabriel, G.; Pawar, R.; Lichtner, P. C.; Wehner, S. C.; Raines, M. A.; Guthrie, G. D., Jr. Analysis and performance of oil well cement with 30 years of CO₂ exposure from the SACROC Unit, West Texas, USA. *Int. J. Greenhouse Gas Control* **2007**, *1*, 75–85.
- (6) Sauman, Z. Carbonization of porous concrete and its main binding components. *Cem. Concr. Res.* **1971**, *1*, 645–662.
- (7) Crow, W.; Carey, J. W.; Gasda, S.; Williams, D. B.; Celia, M. Wellbore integrity analysis of a natural CO₂ producer. *Int. J. Greenhouse Gas Control* **2010**, *4*, 186–197.
- (8) Gasda, S.; Bachu, S.; Celia, M. Spatial characterization of the location of potentially leaky wells penetrating a deep saline aquifer in a mature sedimentary basin. *Environ. Geol.* **2004**, *46*, 707–720.
- (9) Duan, Z.; Sun, R. An improved model calculating CO₂ solubility in pure water and aqueous NaCl solutions from 273 to 533 K and from 0 to 2000 bar. *Chem. Geol.* **2003**, *193*, 257–271.

- (10) Parkhurst, D. L.; Appelo, C. A. J. *User's Guide to PHREEQC (Version 2)—A Computer Program for Speciation, Batch-Reaction, One-Dimensional Transport, And Inverse Geochemical Calculations*, Water-Resources Investigations Report 99-4259; U.S. Geological Survey, 1999; p 310.
- (11) Newell, D. L.; Kaszuba, J. P.; Viswanathan, H. S.; Pawar, R. J.; Carpenter, T. Significance of carbonate buffers in natural waters reacting with supercritical CO₂—Implications for monitoring, measuring and verification (MMV) of geological carbon sequestration. *Geophys. Res. Lett.* **2008**, *35*, L23403 DOI: 10.1029/2008GL035615.
- (12) Linstrom, P. J.; Mallard, W. G. *NIST Chemistry WebBook*, NIST Standard Reference Database Number 69; National Institute of Standards and Technology: Gaithersburg, 2012.
- (13) Gasda, S. E.; Wang, J. Z.; Celia, M. A. Analysis of in-situ wellbore integrity data for existing wells with long-term exposure of CO₂. *Energy Procedia* **2011**, *4*, 5406–5413.
- (14) Kutchko, B.; Strazisar, B. R.; Dzombak, D.; Lowry, G.; Thaulow, N. Degradation of well cement by CO₂ under geologic sequestration conditions. *Environ. Sci. Technol.* **2007**, *41*, 4787–4792.
- (15) Kutchko, B.; Strazisar, B. R.; Huerta, N. J.; Lowry, G.; Dzombak, D.; Thaulow, N. CO₂ reaction with hydrated class H well cement under geologic sequestration conditions. *Environ. Sci. Technol.* **2009**, *43*, 3947–3952.
- (16) Duguid, A.; Scherer, G. W. Degradation of oilwell cement due to exposure to carbonated brine. *Int. J. Greenhouse Gas Control* **2010**, *4*, 546–560.
- (17) Deremble, L.; Loizzo, M.; Huet, B.; Lecampion, B.; Qeusada, D. Stability of a leakage pathway in a cemented annulus. *Energy Procedia* **2011**, *4*, 5283–5290.
- (18) Huet, B.; Prevost, J. H.; Scherer, G. W. Quantitative reactive transport modeling of Portland cement in CO₂-saturated water. *Int. J. Greenhouse Gas Control* **2010**, *4*, 561–574.
- (19) Carey, J. W.; Svec, R.; Grigg, R.; Zhang, J.; Crow, W. Experimental investigation of wellbore integrity and CO₂-brine flow along the casing-cement microannulus. *Int. J. Greenhouse Gas Control* **2010**, *4*, 272–282.
- (20) Huerta, N. J.; Bryant, S. L.; Strazisar, B. R.; Hesse, M. In Dynamic alteration along a fractured cement/cement interface: Implications for long term leakage risk along a well with an annulus defect, *10th International Conference on Greenhouse Gas Control Technologies*, 2011; 2011; pp 5398–5405.
- (21) Liteanu, E.; Spiers, C. Fracture healing and transport properties of wellbore cement in the presence of supercritical CO₂. *Chem. Geol.* **2011**, *281*, 195–210.
- (22) Perrin, J.-C.; Benson, S. An experimental study on the influence of sub-core scale heterogeneities on CO₂ distribution in reservoir rocks. *Transp Porous Med* **2010**, *82*, 93–109.
- (23) Kaszuba, J. P.; Viswanathan, H. S.; Carey, J. W. Relative stability and significance of Dawsonite and aluminum minerals in geologic carbon sequestration. *Geophys. Res. Lett.* **2011**, *38*, L08404.
- (24) Wigand, M.; Kaszuba, J. P.; Carey, J. W.; Hollis, W. K. Geochemical effects of CO₂ sequestration on fractured wellbore cement at the cement/caprock interface. *Chem. Geol.* **2009**, *265*, 122–133.
- (25) Bachu, S.; Bennion, D. B. Experimental assessment of brine and/or CO₂ leakage through well cements at reservoir conditions. *Int. J. Greenhouse Gas Control* **2009**, *3*, 494–501.